

学位論文

Frontal Bone Fracture Patterns Suggesting
Involvement of Optic Canal Damage

香川大学大学院医学系研究科

医学専攻

今城広治

ORIGINAL ARTICLE

Frontal Bone Fracture Patterns Suggesting Involvement of Optic Canal Damage

AQ2

Koji *Imajo*, DDS,* Tomohisa *Nagasao*, MD, PhD,[†] Niyazi *Aizezi*, MD,[†]
Tadaaki *Morotomi*, MD, PhD,[‡] Motoki *Tamai*, MD, PhD,[†] and Minoru *Miyake*, DDS, PhD*

Purpose: Fracture of the frontal bone can be accompanied by damage to the optic canal. The present study uses finite element analysis to identify fracture patterns, suggesting the involvement of the optic canal.

Methods: Ten finite-element skull models were generated from computer tomography data of 10 persons. Then, dynamic analyses simulating collision of a 2-cm-radius brass ball to 6 regions on the frontal bone in the 10 models were performed. Fracture patterns presented by the frontal bone in the 60 experiments were observed, and all those involving the optic canal were selected. Commonalities of the selected fracture patterns were identified.

Results: Fracture of the optic canal was observed in 9 of the 60 patients. In all 9 patients, fracture existed on the anterior and posterior walls of the frontal sinus and on the superior orbital wall.

Conclusion: When the anterior and posterior walls of the frontal sinus and the superior orbital wall are all broken, the optic canal is highly likely to be involved in the damage. When this pattern is observed in emergency examination, preventive decompression of

the optic nerve should be considered to avoid potential occurrence of blindness.

Key Words: Blindness, finite element analysis, fracture, frontal bone, optic canal, orbit, simulation

(*J Craniofac Surg* 2018;00: 00–00)

When the frontal region is strongly struck, the frontal bone can fracture.^{1–5} The anatomical structure of the frontal bone presents inhomogeneity according to location.⁶ Some parts of the frontal bone are thick, and others are thin. Some parts are adjacent to the frontal sinus, and others are not. Because of this structural unevenness, the frontal bone presents various fracture patterns, depending on which part is struck.

Among various fracture patterns, those involving the optic canal need to be treated with great care,⁷ because fracture of the optic canal can cause edema of the optic nerve and subsequent blindness. The present study, using simulation with computer models, aims to identify the patterns of frontal bone fracture wherein the involvement of the optic canal should be suspected.

METHODS

Model Production

Computer tomography (CT) data of the skulls of 10 males (mean \pm SD: 37.5 ± 6.7 years) were collected. The 10 patients had been randomly selected from those who received CT examination of the brain at Kagawa University Hospital for the screening of brain injury after trauma. None of the 10 patients had congenital anomaly of the skull. The usage of their data for the present study was agreed to by the patients, and the study design throughout this study was approved by the institutional review board of Kagawa University.

The CT data in DICOM (Digital Imaging and Communications in Medicine) files were transferred to preprocessor software (Scan IP; Simpleware Ltd, Exeter, UK), where the data were transformed to Standard Triangulated Language files, forming 3-dimensional simulation models of the 10 skulls. The models were divided into 1,450,000 to 1,890,000 tetrahedrally shaped 10-node elements. Appropriate specific density and Young's modulus were assigned to each element. Specific density was calculated by translating Housefield's gray scale⁸; Young's modulus was calculated based on the equation of Kopperdahl ($E = -34.7 + 3230 QCT$), where E and QCT mean Young's modulus (in megapascals) and CT density (in grams per milliliter), respectively.⁹ Thus, 10 models reflecting the accurate shapes and material properties of the original 10 skulls were produced.

Dynamic Simulation of Impact Application

With each of the 10 models, a simulation experiment was conducted in which the frontal bone was struck with a 2-cm-radius brass sphere. We defined 6 round regions on the frontal area of each

From the *Department of Dentistry and Oral Surgery; †Department of Plastic and Reconstructive Surgery, Graduate School of Medicine, Kagawa University; and ‡Department of Plastic and Reconstructive Surgery, Graduate School of Medicine, Kindai University, Ikenobe, Japan.

Received March 11, 2018.

Accepted for publication July 12, 2018.

AQ3

Address correspondence and reprint requests to Tomohisa Nagasao, MD, PhD, Department of Plastic and Reconstructive Surgery, Faculty of Medicine, Graduate School of Medicine, Kagawa University, Kagawa Prefecture, Kida County, Miki-Cho Ikenobe 1750-1, Japan; E-mail: nagasao@med.kagawa-u.ac.jp

This study was approved by the institutional review board of Kagawa University.

The finite element models used in the present study are preserved in digital formats. So the analyses conducted in the study are reproducible.

Part of the present study was supported by a Grant-in-Aid for Scientific Research (C: 15K01292) provided by the Ministry of Education, Culture, Sports, Science and Technology of the Japanese Government.

AQ4

The authors report no conflicts of interest.

Authors' contribution: KI did part of the analyses. TN directed the study and wrote the manuscript. NA corrected CT data for model production. TM provided clinical advice about the meaning of the study. MT reviewed the article. MM provided advice from the standpoint of a dentist.

Example of analysis result showing progress of fracture in response to impact on the IC (Inferior-Central) region (Supplemental Digital Content, <http://links.lww.com/SCS/A359>).

Supplemental digital contents are available for this article. Direct URL citations appear in the printed text and are provided in the HTML and PDF versions of this article on the journal's Web site (www.jcraniofacialsurgery.com).

Copyright © 2018 by Mutaz B. Habal, MD
ISSN: 1049-2275

DOI: 10.1097/SCS.0000000000004926

ORIGINAL ARTICLE

506

Mehr Bildung

популяции? Оцените погрешность.

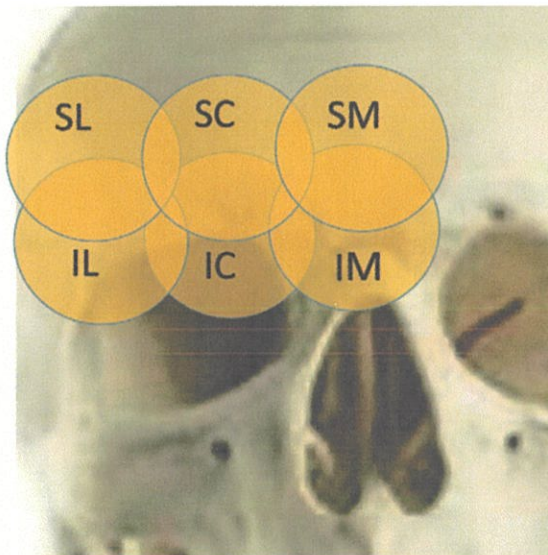


FIGURE 1. For each of the 10 finite-element skull models, 6 regions were defined on the forehead. SL, superior-lateral region; SC, superior-central region; SM, superior-medial region; IL, inferior-lateral region; IC, inferior-central region; IM, inferior-medial region.

AQ5

model: the superior-medial (SM) region, superior-central (SC) region, superior-lateral (SL) region, inferior-medial (IM) region, inferior-central (IC) region, and inferior-lateral (IL) region. The diameter of these 6 regions was defined to be 2 cm, so that the sphere could precisely strike each. These regions are demonstrated in Figure 1.

In a previous study, Waterhouse struck the eyes of cadavers by dropping a brass weight at the velocity of 6 m/s to produce blowout fractures.¹⁰ The impact energy of this experimental condition is 7.4 joules. To produce fractures that could involve not only the orbital wall but also the optic canal, more intense energy must be applied. Hence, in the present study, we arranged the speed of the brass

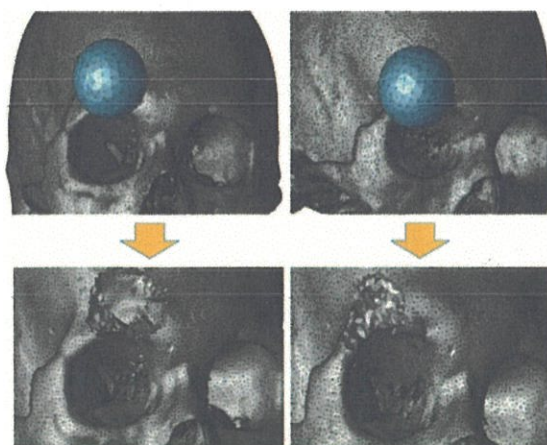


FIGURE 2. Dynamic simulation of impacting the forehead was conducted. The left and right figure pair demonstrates the impact on the superior-central and superior-lateral regions, respectively.

2



FIGURE 3. Examples of resultant fractures in macro view. The acronym on each picture indicates the impacted region. SL, superior-lateral region; SC, superior-central region; SM, superior-medial region; IL, inferior-lateral region; IC, inferior-central region; IM, inferior-medial region.

sphere to produce twice the energy of Waterhouse's experiment. The yield threshold of the bone was assumed to be 150 megapascals.^{8,11} With these experimental conditions, we impacted the frontal bone, and calculated resultant fracture patterns with post-processor software (Livermore Software Technology Corporation, Livermore, CA). Examples of impact application are demonstrated in Figure 2.

Evaluation of Fracture Pattern

The above-stated simulation, striking the 6 regions of each model, produced 6 resultant fractures as shown in Figure 3 (macro view) and Figure 4 (micro view). Since 6 results were obtained for each of the 10 skull models, 60 fracture patients in total were collected. Among the 60 patients, the patients where the optic canal was involved in fracture were identified. For these cases, evaluation was performed regarding the following 3 items.

Region-wise Frequency

Each model was struck at the 6 regions (Fig. 1). For each of the 6 regions, the frequency of presentation of optic-canal fracture was calculated.

Frequencies of Related Position Injury

The frequencies in which fracture involved the nasal bone, medial orbital wall, inferior orbital wall, lateral orbital wall, superior orbital wall, anterior and posterior walls of the frontal sinus, and zygoma were evaluated.

Time-Related Development of Fracture

The LS-DYNA solver allows us to observe the time-related progress of fracture. By using this function, how fracture initiated at the frontal bone came to involve the optic canal was observed.

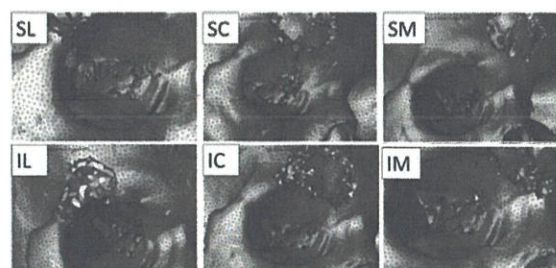


FIGURE 4. Examples of resultant fractures in orbit-focus views. The acronym on each picture indicates the impacted region. SL, superior-lateral region; SC, superior-central region; SM, superior-medial region; IL, inferior-lateral region; IC, inferior-central region; IM, inferior-medial region.

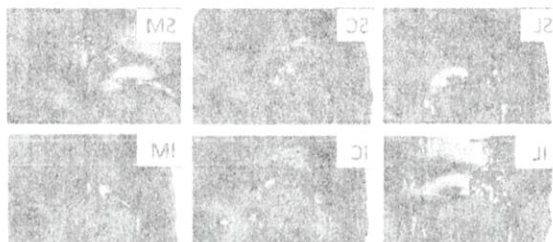


FIGURE 3. Examples of topical zinc acetate ointment technique on rat ear. Top row shows the ear before treatment. Second row shows the ear after topical application of zinc acetate ointment alone (Z), zinc acetate ointment with oil (O), zinc acetate ointment with oil and oil-solubilized zinc acetate (M), zinc acetate ointment with oil and oil-solubilized zinc acetate (C), and zinc acetate ointment with oil and oil-solubilized zinc acetate (L).

dislike of foreign taste the result of *H. pylori* infection, ulcerative colitis, IBD, and so on may contribute to the poor taste of oil. ^{14,15} With zinc acetate ointment (solvent), we injected the solution parenteral route and observed significant increase both *H. pylori* Gastric Gastroesophageal Reflux Disease (GERD) and *C. difficile* colonization rate. ¹⁶ Examples of direct application site dermatopathology are demonstrated in Figure 5.

Evaluation of Fracture Pattern

The 10 rats were randomly assigned to receive oil gelatin or zinc acetate ointment daily for 10 days. Results are shown in Figure 3. Among the 10 zinc acetate oil ointment group, there was no significant difference in fracture rates (mean \pm SEM) compared with the oil gelatin group (5 ± 0.5 vs. 4 ± 0.5 , respectively; $P = 0.5$).

Region-wise Fracture

Fracture regions are shown in Figure 4. There was no significant difference between the distribution of osteoclasts among the four groups ($P > 0.05$).

Distribution of Relative Position Fracture

The distribution of relative position fractures in each region was similar among all four groups (Table 1). There was no significant difference in the number of fractures among the four groups ($P > 0.05$).

Time-Relative Distribution of Fracture

In the 10 rats, the time relative distribution of fractures was similar among all four groups (Table 2). There was no significant difference in the number of fractures among the four groups ($P > 0.05$).

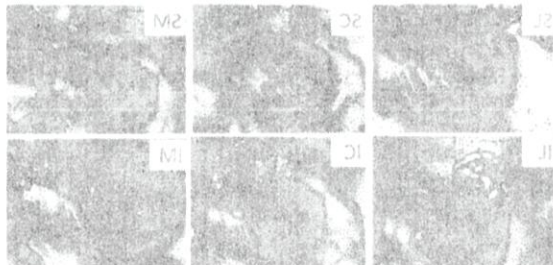


FIGURE 4. Examples of regional fracture patterns in optic-femur mice. Top row shows the femur before treatment. Second row shows the femur after topical application of zinc acetate ointment (Z), zinc acetate ointment with oil (O), zinc acetate ointment with oil and oil-solubilized zinc acetate (M), zinc acetate ointment with oil and oil-solubilized zinc acetate (C), and zinc acetate ointment with oil and oil-solubilized zinc acetate (L).

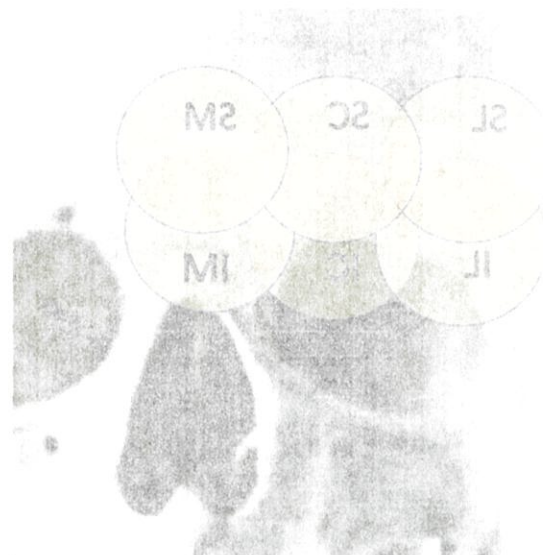


FIGURE 5. Dorsal view of rat hind limb showing hair growth pattern. Top row shows the rat hind limb with normal hair growth. Bottom row shows the rat hind limb with sparse hair growth due to topical application of zinc acetate ointment.

708

regions: the sacroiliac-mobility (SM) region, sacroiliac-center (SC) region, sacroiliac-lateral (SL) region, lateral-mobility (LM) region, and lateral-center (LC) region. The distribution of these six regions was defined to be 6×6 cm² to cover the dorsal surface of the rat. The dorsal surface area of the rat is approximately 10 cm². Therefore, the dorsal surface area of the rat is divided into 10 regions, each of which is approximately 1 cm².

In a previous study, *H. pylori* strains with the ability to bind to the receptors of the intestinal mucosa were found to have a higher incidence of intestinal mucosal damage than those without this ability. ¹⁷ In the present study, *H. pylori* strains with the ability to bind to the intestinal mucosa were found to have a higher incidence of intestinal mucosal damage than those without this ability. ¹⁸ However, in the present study, the ability to bind to the intestinal mucosa was not determined.

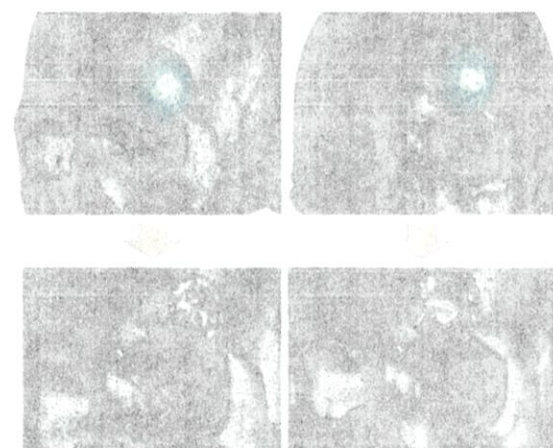


FIGURE 5. Dorsal view of rat hind limb showing hair growth pattern. Top row shows the rat hind limb with normal hair growth. Bottom row shows the rat hind limb with sparse hair growth due to topical application of zinc acetate ointment.

5

AQ1

TABLE 1. Region-wise Frequency of Optic Canal Damage

Impacted Region	Frequency of Optic Canal Involvement
Superior lateral	0
Superior central	7
Superior medial	2
Inferior lateral	0
Inferior central	0
Inferior medial	0

TABLE 2. Involvement of Surrounding Structures in Optic Canal Damage Patients

Regions	Frequency of Optic Canal Fracture
Nasal bone	5
Orbital walls	
Superior wall	9
Medial wall	7
Inferior wall	0
Lateral wall	0
Frontal sinus	
Anterior wall	9
Posterior wall	9
Zygoma	0

RESULTS

Frequency of Optic Canal Involvement

In the 60 patients, fracture of the optic canal occurred in 9 patients.

Region-wise Frequency of Optic Canal Fracture

In the 9 patients with optic canal fracture, the fracture occurred in 7 patients after IC region impact and in 2 patients after SM region impact. Region-wise frequencies are shown in Table 1.

Frequencies of Fractures for Related Positions

Frequencies of fractures for the regions on and around the frontal bone are shown in Table 2. All 9 patients involving the optic canal had fractures on the superior orbital wall and the anterior and posterior walls of the frontal sinus.

Progress of Optic Canal Involvement

In all 9 patients with optic canal involvement, fracture progressed with the same pattern. First, the frontal wall of the frontal sinus broke; then the posterior wall broke; next, the superior orbital wall broke; eventually, fracture reached the optic canal. Time-course fracture development in a patient is shown in Figure 5.

DISCUSSION

The frontal bone breaks when the forehead is strongly impacted. When the intensity of the impact exceeds a certain degree, the fracture is not localized in the frontal bone and extends to surrounding structures, including the cranial base, optic canal, and orbital walls.¹ Damage to these structures can cause liquorhæa,¹² blindness,¹³ and diplopia,¹⁴ respectively. Among these complications, blindness in particular seriously impairs patients' quality of life.

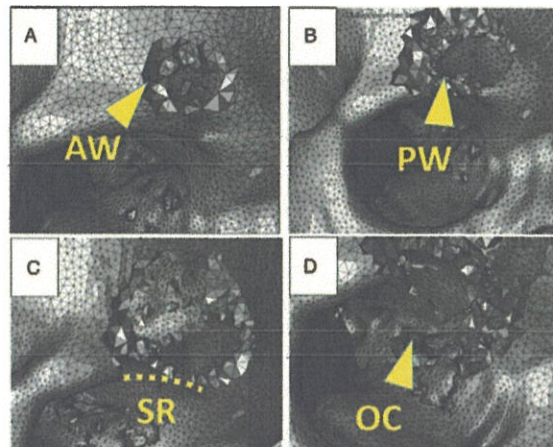


FIGURE 5. Representative pattern of fracture progress. (A) Fracture first occurs on the anterior wall of the frontal sinus (AW). (B) Then the posterior wall of the frontal sinus (PW) breaks. (C) The superior rim of the orbit (SR) breaks. (D) Fracture finally involves the optic canal (OC).

Blindness is caused when injury of the optic canal results in subsequent edema of the optic nerve.

Habal and Maniscalco conducted a minute anatomical study regarding the structure of the optic nerve and classified it into 5 parts: the chiasmatic part, the intracranial part, the inter-canalicular part, the inter-orbital part, and the interocular part.¹⁵ Habal and Maniscalco showed that the optic nerve lies adjacent to the sphenoid plate at the intracranial part, and to the optic canal at the inter-canalicular part. Demonstrating that the optic nerve is tightly surrounded by a bone wall at the inter-canalicular part, Maniscalco and Habal state that the optic canal can be injured in the event of trauma to the front-orbital region, referring to the potential necessity of decompression of the nerve.¹⁶

Hence, in examining trauma of the forehead, it is necessary to diagnose whether or not the optic canal is injured. Believing that identification of fracture patterns wherein injury of the optic canal is likely to occur is useful to making more precise diagnoses, we have undertaken the present study.

Finite-element simulation was used in the present study. Finite-element simulation is an established technique for medical research, and is used to clarify the biomechanical behaviors of such organs as facial bones,¹⁷ thoraces,¹⁸ and skin.¹⁹ We employed finite-element simulation in the present study, because it guarantees accuracy of experimental conditions. In most previous studies regarding the mechanisms of facial bone fracture, actual human skulls were impacted, and resultant fracture patterns were observed.^{20–22} With such methods, reproducibility and accuracy of the experimental conditions cannot be guaranteed because of instability of the conditions of impact application. In addition, ethically speaking, damaging actual human skulls is unacceptable in the 21st century. Finite-element simulation is advantageous from these standpoints, because it not only guarantees accuracy of experimental conditions but also has few ethical problems.

Human skulls vary in shape and hardness. Because of individual differences, a finding with 1 skull is not necessarily true for others. To avoid this problem and increase the generality of the findings, we performed the same set of experiments (brass-sphere impacting on 6 regions) with 10 skull models. Evaluation with 10 models improves the reliability of the findings.

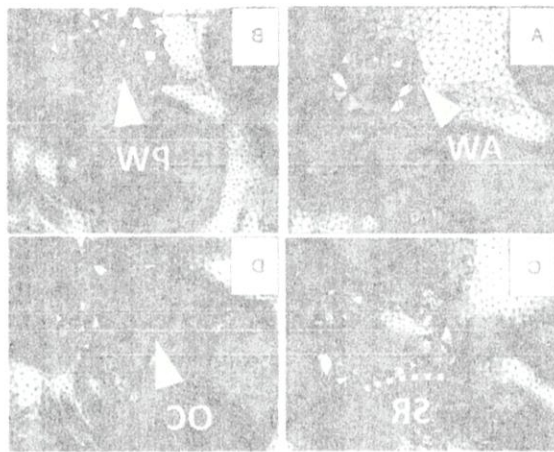


FIGURE 8. Six grayscale images showing the initial state of the environment (A), the state after moving the white triangle to the position shown in (A) (B), the state after moving the black rectangle labeled 'WA' to the position shown in (B) (C), the state after moving the black rectangle labeled 'PM' to the position shown in (D) (E), and the final state (F).

Ridgeless regression is chosen after trying all the other linear models in Ridge and Alternating direction subgradient optimization shows a minimum loss function than

least squares and ridge regression in terms of the total error and also has better convergence properties than gradient descent. Ridge regression has the same computational cost as least squares but is more robust to outliers. Ridge regression can be used to find the best fit line for a given set of data points by minimizing the sum of the squared residuals plus a regularization term. Ridge regression is often used in the field of machine learning for feature selection and dimensionality reduction. It helps to reduce overfitting and improves the generalization performance of the model.

Hence, in this work, we have used ridge regression to find the relationship between the independent variables and the dependent variable. Ridge regression is a type of linear regression that applies a penalty to the coefficients of the independent variables. This helps to reduce overfitting and improves the generalization performance of the model.

In this experiment, we have used ridge regression to find the relationship between the independent variables and the dependent variable. Ridge regression is a type of linear regression that applies a penalty to the coefficients of the independent variables. This helps to reduce overfitting and improves the generalization performance of the model. Ridge regression is a type of linear regression that applies a penalty to the coefficients of the independent variables. This helps to reduce overfitting and improves the generalization performance of the model. Ridge regression is a type of linear regression that applies a penalty to the coefficients of the independent variables. This helps to reduce overfitting and improves the generalization performance of the model.

Hence, in this work, we have used ridge regression to find the relationship between the independent variables and the dependent variable. Ridge regression is a type of linear regression that applies a penalty to the coefficients of the independent variables. This helps to reduce overfitting and improves the generalization performance of the model.

Region-Wise Frequency of Object Class per frame	Frequency of Object Class per frame
0	Initial
0	Intermediate
0	Final
0	Initial
0	Intermediate
0	Final

Region-Wise Frequency of Object Class per frame	Frequency of Object Class per frame
0	Initial
0	Intermediate
0	Final
0	Initial
0	Intermediate
0	Final

RESULTS

Frequency of Object Class Initial

Region-Wise Frequency of Object Class Initial

Region-Wise Frequency of Object Class Intermediate

Region-Wise Frequency of Object Class Final

Properties of Object Class Intermediate

Properties of Object Class Final

DISCUSSION

The following table shows the frequency of each object class in the intermediate frame. The frequency of each object class in the intermediate frame is as follows:

Object Class	Frequency
WA	1
PM	1
OC	1

Besides the accuracy of the experimental conditions, another methodologic advantage of finite-element simulation is that it enables observation of the progress of the fracture. In previous studies on actual human skulls, only the final condition of the fracture was observable; the process by which the fracture advances was unobservable due to the brevity of the time of impact application. On the contrary, with finite-element simulation, the progress of fracture can be observed at any moment (Fig. 5), by halting calculation. This function enables observation of how fracture initiated at the frontal bone advances to surrounding structures.

In all 9 patients where the optic canal was damaged, fracture first occurred at the frontal sinus, progressing to the upper orbital wall, and eventually breaking the optic canal (Fig. 6). This pattern, where the fracture continuously progresses from the directly impacted site to the opposite side, may appear a matter of course and unworthy of discussion. However, this pattern is not necessarily the case with other fractures. For instance, when the region around the infra-orbital foramen is impacted, the directly impacted site and the inferior orbital wall may fracture. However, the inferior orbital rim, the structure between the 2 sites, often remains unbroken. This characteristic fracture pattern is given the special name "blowout fracture." Before performing this study, we had expected a similar phenomenon might occur with frontal bone fractures, presenting discontinuity between fractures at the frontal sinus and the optic canal, without the destruction of the upper orbital wall. However, such an enclave-like fracture pattern occurred in none of the 9 patients. In all patients where the optic canal was damaged, fracture occurred presenting a continuously progressive pattern.

In all 9 patients showing damage of the optic canal, fracture involved the anterior/posterior walls of the frontal sinus and the upper orbital wall. Inductive evaluation of this finding allows us to propose a diagnostic protocol: "When the anterior/posterior walls of the frontal sinus and the upper orbital wall are broken, the optic canal is highly likely to be involved in the damage, so injury should be suspected." This diagnostic protocol is useful in screening for optic canal injury at emergency rooms.

When the optic canal is injured, decompression of the optic nerve should be performed as soon as possible to prevent edema of the optic nerve and subsequent blindness. To perform this early stage prevention, damage to the optic canal must be screened for immediately after injury. However, identification of optic canal damage in an emergency room is often challenging for the following 2 reasons. First, the patient is often unconscious, so physicians cannot examine the patient's visual function. Second, the fracture of the optic canal is often too subtle, presenting only small slits, to be found in low resolution computer-tomographic images. Hence, in early stage screening, the fracture can go undetected.

The given diagnostic protocol works to reduce such misjudgment. When evident fracture is observed in the previously stated 3

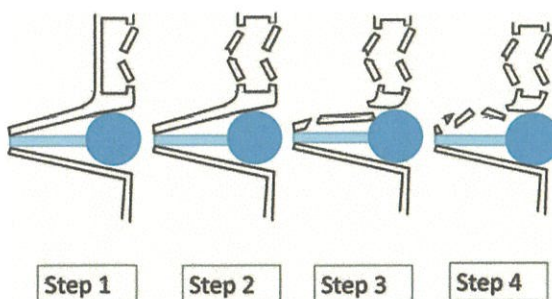


FIGURE 6. Schematic demonstration of fracture progress pattern.

structures (the anterior and posterior walls of the frontal sinus, and the upper orbital wall), the optic canal is likely to be damaged too, even if the damage is not evident. In such situations, the optic canal should be re-examined with computer tomography at a higher resolution, and double checked by a team of physicians. By taking such care, the occurrence of blindness can be prevented.

The present study focused on mechanisms of frontal bone fracture. However, besides the frontal bone, fracture also occurs frequently on other facial bones, such as the zygoma, upper jaw, and nasal bone. We plan to extend our study to include these bones to clarify diagnostic protocols regarding these bones. We believe accumulation of such diagnostic protocols will greatly contribute to the accuracy of diagnosis of facial bone fractures.

Furthermore, recent advancement of microscopic and endoscopic surgical techniques enables surgeons to access the tissues around the optic canal and the cavernous sinus more accurately and effectively than in the past.^{23,24} Accordingly, the necessity of evaluating damage to these structures in traumatic situations is increasing. In the present study, the damage to the optic canal was observed at the macro level. However, since the optic canal is a subtle anatomical structure, minor damage, even on scales <1 mm, can cause edema of the optic nerve and impair it. Hence, we plan to expand our studies to elucidate micro-level damage of the optic canal in traumatic situations in our future studies.

CONCLUSION

By using finite-element simulation, the present study analyzed various fracture patterns of the frontal bone. In 60 patients with dynamic simulation with 10 skull models, the optic canal was injured in 9 patients. All the 9 patients had fracture of the anterior and posterior walls of the frontal sinus and of the upper orbital wall in common. Inductive reference of this finding suggests a diagnostic protocol: "When the anterior and posterior walls of the frontal sinus and the upper orbital wall are broken, fracture of the optic canal should be suspected." Clinical application of this protocol in emergency diagnosis facilitates accurate screening of optic canal damage, and contributes to prevention of possible blindness.

ACKNOWLEDGMENT

The authors extend their gratitude to Shingo Kagawa and Miki Miyazaki at JSOL Co (Tokyo, Japan) for their technical support in finite element analyses in the present study.

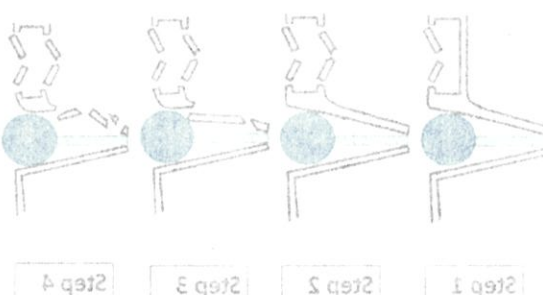
REFERENCES

1. Weitman E, Shilo D, Emodi O, et al. Solitary frontal sinus fractures compared to multiple facial fractures, energy impact dependency. *J Craniofac Surg* 2017;28:1812–1815
2. Kim YW, Lee DH, Cheon YW. Secondary reconstruction of frontal sinus fracture. *Arch Craniofac Surg* 2016;17:103–110
3. Schultz K, Braun TL, Truong TA. Frontal sinus fractures. *Semin Plast Surg* 2017;31:80–84
4. Winston KR, Beauchamp K, Harasaki Y. Everting fracture of entire frontal bone: management and importance of preliminary reconstruction. *J Craniofac Surg* 2017;28:1090–1092
5. Florentin VG, Mendonça DS, Bezerra AV, et al. Reconstruction of frontal bone with custom-made prosthesis using rapid prototyping. *J Craniofac Surg* 2016;27:e354–e356
6. May H, Mali Y, Dar G, et al. Intracranial volume, cranial thickness, and hyperostosis frontalis interna in the elderly. *Am J Hum Biol* 2012;24:812–819
7. Urolagin SB, Kotashetti SM, Kale TP, et al. Traumatic optic neuropathy after maxillofacial trauma: a review of 8 cases. *J Oral Maxillofac Surg* 2012;70:1123–1130
8. Huempfner-Hierl H, Schaller A, Hemprich A, et al. Biomechanical investigation of naso-orbitoethmoid trauma by finite element analysis. *Br J Oral Maxillofac Surg* 2014;52:850–853

Conclusion

ACKNOWLEDGMENT

REFERENCES



9. Kopperdahl DL, Pearlman JL, Keaveny TM. Biomechanical consequences of an isolated overload on the human vertebral body. *J Orthop Res* 2000;18:685-690
10. Waterhouse N, Lyne J, Urdang M, et al. An investigation into the mechanism of orbital blowout fractures. *Br J Plast Surg* 1999;52:607-612
11. Nagasao T, Miyamoto J, Nagasao M, et al. The effect of striking angle on the buckling mechanism in blowout fracture. *Plast Reconstr Surg* 2006;117:2373-2380
12. Raveh J, Stich H, Schawalder P, et al. Biocement - a new material. Results of its experimental use for osseous repair of skull cap defects with lesions of the dura mater and liquorhea, reconstruction of the anterior wall of the frontal sinuses and fixation of alloimplants. *Acta Otolaryngol* 1982;94:371-384
13. Adetayo OA, Naran S, Bonfield CM, et al. Pediatric cranial vault fractures: analysis of demographics, injury patterns, and factors predictive of mortality. *J Craniofac Surg* 2015;26: 1840-1846
14. Metzinger SE, Guerra AB, Garcia RE. Frontal sinus fractures: management guidelines. *Facial Plast Surg* 2005;21:199-206
15. Habal MB, Maniscalco JE. Surgical relations of the orbit and optic nerve: an anatomical study under magnification. *Ann Plast Surg* 1980;4:265-275
16. Maniscalco JE, Habal MB. Microanatomy of the optic canal. *J Neurosurg* 1978;48:402-406
17. Nagasao T, Miyamoto J, Jiang H, et al. Interaction of hydraulic and buckling mechanisms in blowout fractures. *Ann Plast Surg* 2010;64:471-476
18. Nagasao T, Noguchi M, Miyamoto J, et al. Dynamic effects of the Nuss procedure on the spine in asymmetric pectus excavatum. *J Thorac Cardiovasc Surg* 2010;140:1294-9.e1
19. Nagasao T, Hamamoto Y, Tamai M, et al. The "Sea" should not be operated on in scar revision for "Island-Like" scars. *Med Hypotheses* 2015;85:215-218
20. Ahmad F, Kirkpatrick NA, Lyne J, et al. Buckling and hydraulic mechanisms in orbital blowout fractures: fact or fiction? *J Craniofac Surg* 2006;17:438-441
21. Fujino T, Sugimoto C, Tajima S, et al. Mechanism of orbital blowout fracture. II. Analysis by high speed camera in two dimensional eye model. *Keio J Med* 1974;23:115-124
22. Tajima S, Fujino T, Oshiro T. Mechanism of orbital blowout fracture. I. Stress coat test. *Keio J Med* 1974;23:71-75
23. Joo W, Funaki T, Yoshioka F, et al. Microsurgical anatomy of the carotid cave. *Neurosurgery* 2012;70:300-311
24. Martins C, Costa E, Silva IE, et al. Microsurgical anatomy of the orbit: the rule of seven. *Anat Rec Int* 2011;2011:468727

SCS**Journal of Craniofacial Surgery****Manuscript No. SCS-18-0481**

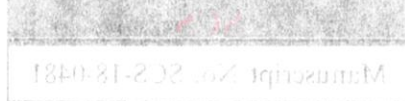
Dear Author,

During the preparation of your manuscript for typesetting, some queries have arisen. These are listed below. Please check your typeset proof carefully and mark any corrections in the margin as neatly as possible or compile them as a separate list. This form should then be returned with your marked proof/list of corrections to the Production Editor.

QUERIES: to be answered by AUTHOR

QUERY NO.	QUERY DETAILS	RESPONSE
<AQ1>	As per style, the short title/running head can have a maximum of 40 characters including spaces, and abbreviations/acronyms only as exceptions. Please check the suggested short title, " <i>Frontal Bone Fractures</i> " for appropriateness.	
<AQ2>	Please confirm whether surnames/family names (red) have been identified correctly in the author byline.	
<AQ3>	Please check the accuracy of corresponding author information.	
<AQ4>	Please verify the accuracy of both the author affiliations section and the conflicts of interest section.	
<AQ5>	If you have color in your proof, please indicate whether you approve the color charge by returning the color agreement with your corrections. The color agreement can be found at http://links.lww.com/SCS/A52 . The price for the first color figure is \$400. The charge for each additional color figure is \$100. If you prefer black and white figures, please indicate so on your proof corrections.	

Journal of Chiropractic Studies



Dear Author

During the preparation of your manuscript for submission, some choices have arisen. Please see the following points. Please check how these may affect your submission in the manner described below. This form should help you to interact with your manuscript thoroughly before or during your first revision. This form should also assist you in the preparation of your manuscript.

OFFER NO.	OFFER DETAILS	RESPONSE
>AO1<	A 4-page spread (one side) containing 1 page can place a maximum of 40 characters including spaces and punctuation.	Please consider this as exception. Please check the following section titled "Format".
>AO2<	A 4-page spread (one side) containing 1 page can place a maximum of 40 characters including spaces and punctuation.	Please consider this as exception. Please check the following section titled "Format".
>AO3<	Please check the second of the following sections: "Author Information" or "Section of the paper".	Please check the second of the following sections: "Author Information" or "Section of the paper".
>AO4<	Please check the second of the following sections: "Author Information" or "Section of the paper".	Please check the second of the following sections: "Author Information" or "Section of the paper".
>AO5<	If you have color in your final print please indicate which color you will use for the illustrations. If the color is not found in print, it can be found in print.	If you have color in your final print, please indicate which color you will use for the illustrations. If the color is not found in print, it can be found in print.
>AO6<	The price for color prints is \$100. The charge for black and white prints is \$100.	The price for color prints is \$100. The charge for black and white prints is \$100.
>AO7<	If you want additional color prints, the charge is \$100.	If you want additional color prints, the charge is \$100.
>AO8<	If you want additional prints, the charge is \$100.	If you want additional prints, the charge is \$100.
>AO9<	If you want additional prints, the charge is \$100.	If you want additional prints, the charge is \$100.
>AO10<	If you want additional prints, the charge is \$100.	If you want additional prints, the charge is \$100.